Viscous Drag Reduction by Periodic Acceleration & Deceleration

Yair Reingewirtz,[1] Yakov Paley[2] and David Greenblatt[3]
Technion – Israel Institute of Technology, Technion City, Haifa 3200003, Israel

1 Introduction

The field of viscous aerodynamic drag reduction includes a wide variety of passive and active methods that mostly aim to manipulate near-wall coherent turbulent motions [1]. Certain methods, not considered to be viable on manned vehicles, may be viable on unmanned vehicles that are not constrained by human comfort or physiological limitations [2]. One such method is non-harmonic, periodic, acceleration and deceleration of the vehicle, possibly attained by intermittent propulsion. This approach is based on observations of net drag and pumping power savings in non-harmonic, periodic, internal (pipe and channel) flows [3-9]. For example, direct numerical simulations (DNS) with short-duration pulse-modulation of the pressure gradient, show an energy saving of around 30% [8]; and a combined experimental-computational study employing an asymmetric triangular waveform followed by a "diastolic" rest phase show a drag reduction of more than 25% [9]. In these flows, there are at least two drag reduction mechanisms: rapidly accelerated turbulent flows tend to "relaminarize," thereby producing relatively low skin friction [10-17]; while decelerated flows produce lower skin friction due to the adverse temporal pressure gradient.

The objective of this research is to study the rapid temporal acceleration and deceleration of a nominally incompressible turbulent flat plate boundary layer, to determine if a net skin friction drag reduction can be realized. The experiment is conducted on a flat plate with a leading-edge trip, in an unsteady wind tunnel, where flow deceleration and acceleration are achieved by closing and opening a set of downstream louver vanes. In this preliminary study, the evaluation is performed by comparing the local ensemble-averaged skin friction coefficients $c_f' \equiv \tau_w / q_\infty$ with their corresponding quasi-steady values. Details of the experimental setup are described in section 2; the results, discussion and scaling considerations are presented in section 3; and the conclusions are summarized in section 4. This preliminary

---

[1] Undergraduate student, Faculty of Mechanical Engineering.
[2] Laboratory Engineer, Danciger Undergraduate Laboratories, Faculty of Mechanical Engineering.
[3] Professor, Faculty of Mechanical Engineering, AIAA Associate Fellow, davidg@technion.ac.il.

study does not directly consider specific modulated or intermittent propulsion methods or techniques that would be required to achieve periodic vehicle acceleration and deceleration.

2 Experimental Setup

Experiments were performed in a blower-type unsteady wind tunnel, with an 8:1 contraction and a 250 × 152.5 mm test section; it is a ¼ scaled-down version of the unsteady wind tunnel described in [23] (see Fig. 1). A set of counter-rotating louver vanes, driven by a pneumatic actuator, are mounted at the tunnel exit. With the louver vanes installed, the maximum freestream velocity U_∞ is 50 m/s and the turbulence levels is 3.9%.

A 5 mm thick, 350 mm long aluminum flat plate, with an elliptical leading-edge and a trailing-edge flap, was mounted in the center of the test section, 100 mm downstream of the contraction. A leading-edge trip (120-grit sandpaper roughness) was wrapped around the elliptical leading-edge and extended 10 mm on both surfaces. All experiments were performed at a fixed fan speed: steady experiments were performed by statically varying the vane angles; and unsteady experiments were performed by rapid partial closing of the vanes, followed by rapid opening after 1,000 ms.

Fifteen pressure ports, with a 20 mm spacings between them, were installed on the one wall of the tunnel, and connected to 5 inH_2O (1.27 kPa) Honeywell HSC differential pressure transducers, using close-coupled vinyl tubing, as shown in Fig. 1. Prior to, and following experiments, the pressure transducers were calibrated using an inclined-tube alcohol-based manometer. The steady and unsteady pressure gradients (dp/dx and $\partial p/\partial x$) were obtained by means of least-squares linear curves. Velocity and skin friction measurements were made using a right angle hot-wire probe (Dantec 55P14) and a flush-mounted hot film (Dantec 55R47), respectively, in conjunction with an AA Lab Systems hot wire anemometer. All probes were located at x_m = 265 mm downstream of the leading-edge, where the hot-film sensor was displaced 50 mm in the cross-stream direction. A pitot-static probe (Dwyer model 166-12), with an inclined-tube alcohol-based manometer was used to calibrate the probes (but removed for experiments), by statically varying the louver vanes. Fifty unsteady measurements were performed and the resulting data were ensemble-averaged, which resulted in <1% precision for velocity and skin friction measurements based on 95% confidence intervals. The measurement of steady flow velocity profiles $u = u(y)$ showed close correspondence with standard log-law and power-law relationships. Skin friction was calibrated by means of the well-known correlation $c'_f = 0.0576(U_\infty x_m / \nu)^{-1/5}$ [24].

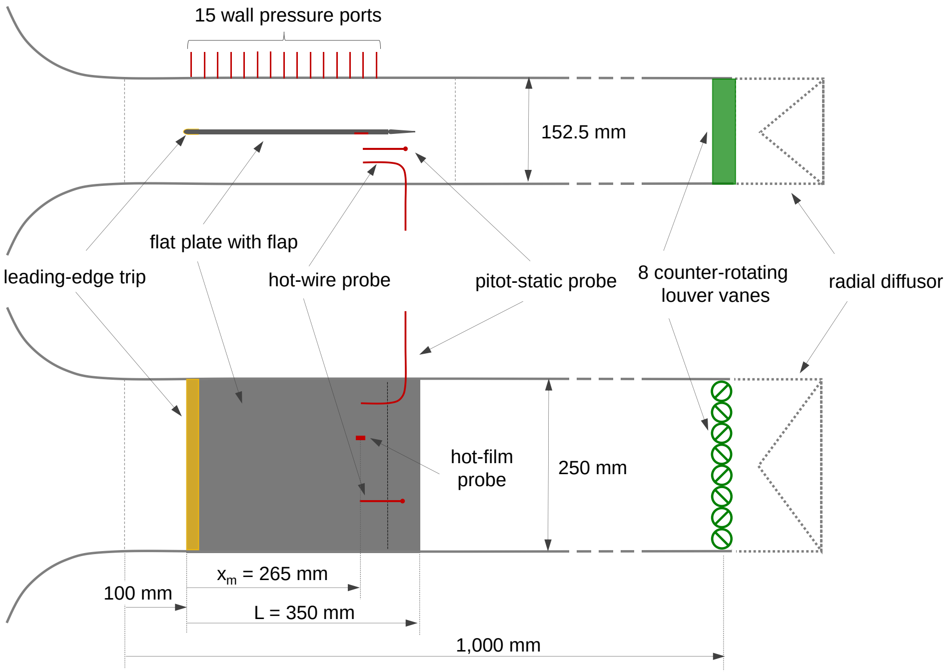

Fig. 1 Schematic of the experimental setup showing top (above) and side (below) views of the wind tunnel test section, flat plate setup, main dimensions and measurement instrumentation.

3 Results and Discussion

Ensemble-averaged results of hot wire velocity and test section pressure are shown in Fig. 2, for the louver vanes closing and opening sequentially, with insets showing the deceleration and acceleration details. As expected, flow speed control using the vanes clearly produces a higher test section pressures at lower speeds. More surprising, however, is the large impact of compressibility; both for the acceleration and deceleration, despite the nominally incompressible conditions ($Ma < 0.1$). During deceleration, i.e., rapid partial closing of the vanes, large pressure oscillations (in excess of the 1.27 kPa transducer range) are observed that closely correspond to the Helmholtz frequency of 29 Hz [23], i.e., the nominally isentropic compression and expansion in the plenum. The local freestream deceleration then lags the initial pressure increase by approximately 54 ms. During acceleration, i.e., rapidly opening of the vanes, the Helmholtz effect is greatly reduced but the velocity lags the pressure by approximately 47 ms, again, due to compressibility. Therefore, unlike incompressible (liquid) pipe and channel flows [4-17,19-22] we cannot rely on the incompressibility assumption $\rho dU_\infty / dt = -\partial p / \partial x$, to infer the temporal acceleration from the pressure gradient. Under harmonic oscillations at similar frequencies $(\approx 1 \text{ Hz})$, compressibility effects are significantly reduced [23].

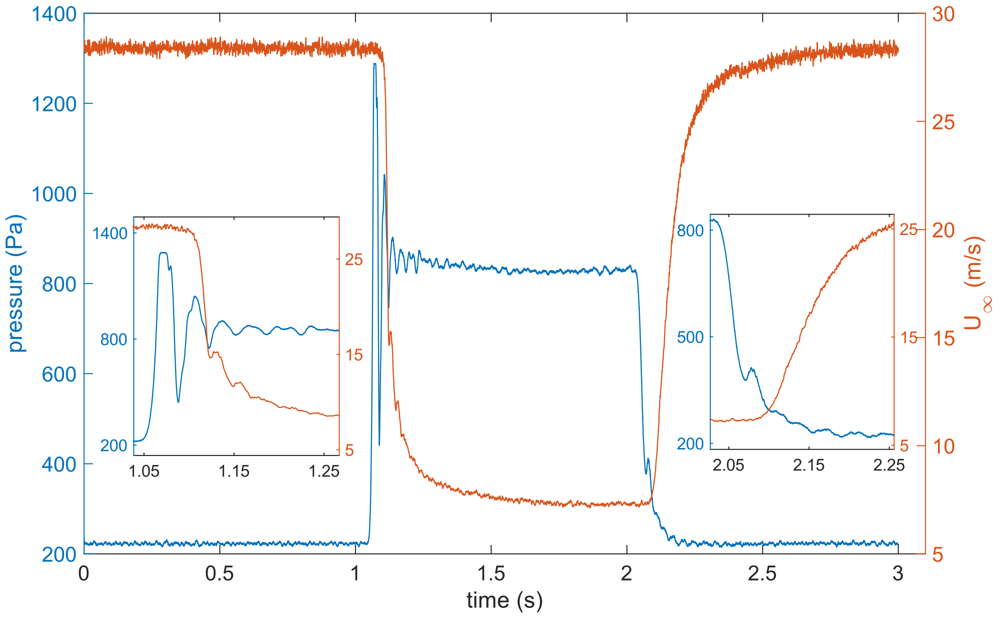

Fig. 2 Ensemble-averaged test section pressure and freestream velocity during rapid closing and opening of the downstream louver vanes. Insets show details of the initial stages.

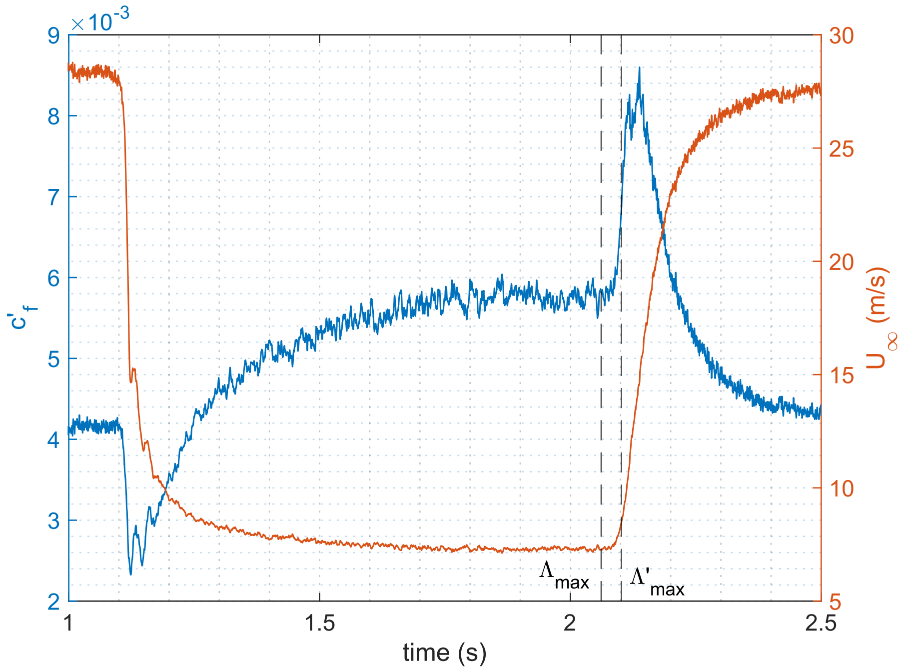

Fig. 3 Ensemble-averaged skin friction coefficient and free stream velocity during the deceleration and acceleration phases. Times corresponding to $\Lambda_{max} = 17.5$ and $\Lambda'_{max} \equiv 5.1$ are indicated.

Ensemble-averaged skin friction coefficient and freestream velocity are shown in Fig. 3, corresponding to the interval $1\text{ s} \le t \le 2.5\text{ s}$ of Fig. 2. Much like rapidly decelerated pipe and channel flows, the skin friction coefficient decreases sharply with decreasing velocity. This is explained principally as an inertia effect [19,21], i.e., the velocity profile decreases almost uniformly (like a plug-flow in pipes), apart from the region very near the wall, which leads to a significant reduction in wall shear stress. Following this, c_f' exhibits high frequency oscillations, that correspond to the Helmholtz-oscillation-induced freestream oscillations. These velocity oscillations are relatively small, but it can be expected that a lower c_f' minimum would be attained if they were absent. A welcome result is that the skin friction coefficient does not exceed its final steady state value as observed in pipe and channel flows [19-22]. The most likely reason is that in our experiments the latter part of the deceleration is gradual, whereas in pipe and channel flow studies, the deceleration typically ends abruptly, with a piecewise continuous bulk flow velocity U_b. This acceleration singularity corresponds to a sharp c_f' minimum, which can go negative to produce skin friction thrust [22], followed by an overshoot of the final value [19,21] that can take up to 800 viscous time units to recover [21]. Thus, in contrast to prior pipe flow results, the present deceleration phase corresponds to a net decrease in drag coefficient when compared to the quasi-steady value. Note, in addition, that our deceleration phase of $t = 1\text{ s}$ is comparable to that of pulse-modulated pumping [8], based in near-wall scaling, namely $16,200\nu / u_{\tau 0}^2 \approx 1.8\text{ s}$.

The acceleration phase is characterized by a rapid increase in c_f', similar to pipe and channel flows and, again, this is explained as an inertial effect where the velocity profile increases almost uniformly [13,17]. An important difference, however, is that c_f' does not drop below its corresponding quasi-steady value, but rather diminishes gradually towards its final state. The absence of relaminarization can be explained by generalizing the criterion of [18], by including temporal acceleration effects, namely $\Lambda \equiv -\partial p / \partial x / (\tau_w / \delta) > 50$ which represents the dominance of pressure forces over the Reynolds shear forces, irrespective of whether the pressure gradient is spatial or temporal. However, the pressure gradient peak occurs *prior* to the flow acceleration, and thus we are compelled to use an "equivalent local incompressible pressure gradient" $-\rho dU_\infty / dt$ and hence an effective relaminarization parameter $\Lambda' \equiv (\rho dU_\infty / dt) / (\tau_w / \delta)$. The peak values, namely $\Lambda_{\max} = 17.5$ and $\Lambda'_{\max} \equiv 5.1$, are indicated on Fig. 3, where the latter is an order of magnitude less than that required for relaminarization. This observation is consistent with the acceleration time interval described in [8], for which the bulk velocity increases by a factor of 16 over $1{,}800\nu / u_{\tau 0}^2 = 200\ \mathrm{ms}$, which is roughly an order of magnitude greater than that in our experiment. Lower acceleration rates may be sufficient to produce relaminarization in the case of natural transition, in that the stabilizing effect of the pressure gradient could result in transition occurring at significantly higher Reynolds numbers (cf. [25]). This can be examined by repeating the present experiment with the transition trip removed.

The data of Fig. 3 are summarized parametrically according to their corresponding Reynolds number and shown together with steady data and the flat plate skin friction coefficient correlation in Fig. 4. As anticipated, the acceleration only produces an overshoot and the deceleration only produces and undershoot of the quasi-steady results. On the basis of these data, a strategy can be developed to achieve a net drag reduction, based on quasi-steady acceleration, followed by a relatively rapid deceleration. One could devise such an experiment, for example, using a towing tank with unsteady capabilities [26].

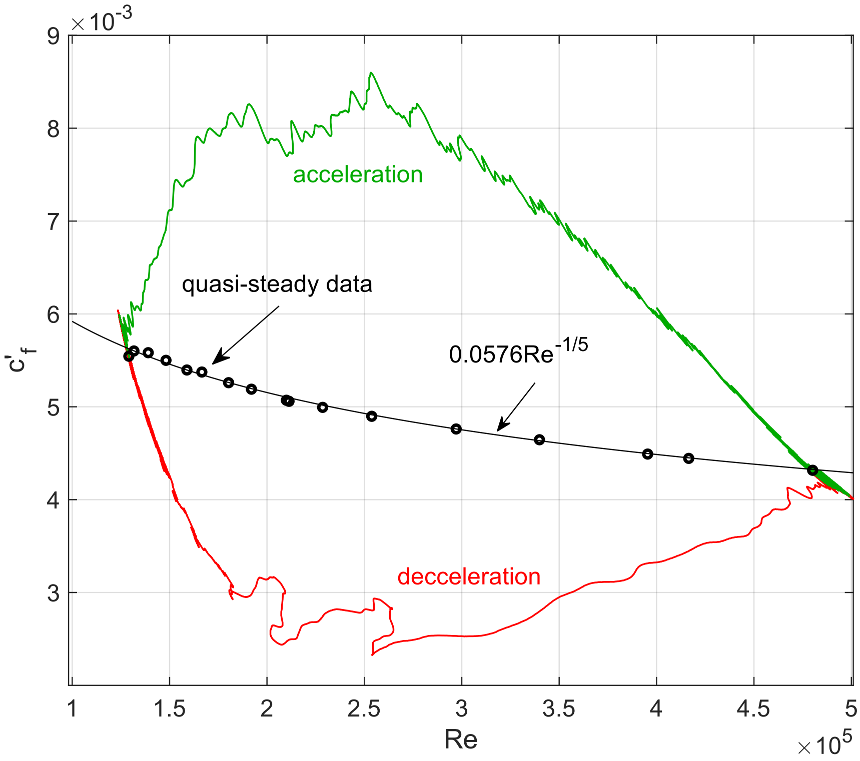

Fig. 4 Parametric plot of skin friction coefficient as a function of corresponding Reynolds number, showing deceleration and acceleration phases relative to corresponding quasi-steady values.

While viscous drag reduction can clearly be achieved, this must translate to propulsive energetic savings on an unmanned vehicle. In internal flows, low duty-cycle (~10%), pulse-modulated pumping [8], i.e., rapid constant acceleration over ~10% of the cycle, followed by slower deceleration over ~90% of the cycle, can produce an energetic saving. The equivalent strategy on a vehicle involves pulse-modulated, or intermittent, propulsion using a comparably low duty cycle. To attain relaminarization, however, our data together with that of [7-17], show that extremely high acceleration rates must be attained, typically $\text{g-force} = O(10)$, although lower acceleration rates could be achieved with an initially laminar boundary, where transition is delayed due to the acceleration (cf. [25,27]). Note furthermore that while viscous drag is the only internal-flow retarding force, pressure drag, induced drag and added mass effects must be accounted for on lift-producing vehicles. Development of such vehicles may require new approaches to propulsion-system, aerodynamic and structural design.

4 Conclusions

An experimental wind tunnel study was performed to investigate the viability of incompressible turbulent boundary layer skin friction drag reduction by temporal acceleration and deceleration, motivated by similar pipe and channel flows studies. The acceleration and deceleration phases were achieved by rapidly opening and closing a set of downstream louver vanes, and it was observed that wind tunnel compressibility effects are substantial despite the nominally incompressible conditions. Deceleration produced an undershoot of the corresponding quasi-steady flow, but did not subsequently overshoot like in pipe flows due gradual reduction of the deceleration. The acceleration phase exhibited a skin friction coefficient overshoot, but did not subsequently produce the well-known relaminarization undershoot, due to a weaker and insufficiently-sustained acceleration. Energetic savings can potentially be achieved by intermittent propulsion that produces rapid acceleration over a small fraction of the cycle, followed by relatively slow deceleration for the remainder of the cycle.

References

1. Corke, T.C. and Thomas, F.O., “Active and passive turbulent boundary-layer drag reduction,” *AIAA Journal*, Vol. 56, No. 10, 2018, pp. 3835-3847. https://doi.org/10.2514/1.J056949.

2. Greenblatt, D. and Williams, D.R., “Flow control for unmanned air vehicles,” *Annual Review of Fluid Mechanics*, Vol. 54, 2022, pp. 383-412. https://doi.org/10.1146/annurev-fluid-032221-105053.
3. Iwamoto, K., Sasou, N. & Kawamura, H. “Direct numerical simulation of pulsating turbulent channel flow for drag reduction,” Advances in Turbulence XI, Springer Proceedings Physics, Vol 117. Springer, Berlin, Heidelberg, eds: J.M.L.M. Palma and A.S. Lopes, 2007, pp. 709-711. https://doi.org/10.1007/978-3-540-72604-3_225.
4. Souma, A., Iwamoto, K. and Murata, A., “Experimental investigation of pump control for drag reduction in pulsating turbulent pipe flow,” Sixth International Symposium on Turbulence and Shear Flow Phenomena, Seoul, Korea, 2009, pp. 2761-2765. https://doi.org/10.1615/TSFP6.1220.
5. Ciofalo, M., “Reducing Pumping Power Consumption by Pulsed Operation?” *Journal of Fluids Engineering*, Vol. 144, No. 12, 2022, p. 124501. https://doi.org/10.1115/1.4055170.
6. Kobayashi, W., Shimura, T., Mitsuishi, A., Iwamoto, K. and Murata, A., “Prediction of the drag reduction effect of pulsating pipe flow based on machine learning,” *International Journal of Heat and Fluid Flow*, Vol. 88, 2021, p.108783. https://doi.org/10.1016/j.ijheatfluidflow.2021.108783.
7. Rota, G.F., Monti, A., Rosti, M.E. and Quadrio, M., “Saving energy in turbulent flows with unsteady pumping,” *Scientific Reports*, Vol. 13, No. 1, 2023, p.1299.977. https://doi.org/10.1038/s41598-023-28519-x.
8. Rota, G.F., Monti, A., Rosti, M.E. and Quadrio, M., “On-off pumping for drag reduction in a turbulent channel flow,” *Journal of Fluid Mechanics*, Vol. 966, A12-1-12, 2023, http://doi.org/10.1017/jfm.2023.451.
9. Scarselli, D., Lopez, J.M., Varshney, A. and Hof, B., “Turbulence suppression by cardiac-cycle-inspired driving of pipe flow,” *Nature*, Vol. 621, No. 7, 2023, pp. 71-74. https://doi.org/10.1038/s41586-023-06399-5.
10. Shuy, E.B., “Wall shear stress in accelerating and decelerating turbulent pipe flows,” *Journal of Hydraulic Research*, Vol. 34, No. 2, 1996, pp. 173-183. https://doi.org/10.1080/00221689609498495.
11. Greenblatt, D. and Moss, E.A., “Pipe-flow relaminarization by temporal acceleration,” *Physics of Fluids*, Vol. 11, No. 11, 1999, pp. 3478-3481. https://doi.org/10.1063/1.870205.

12. Greenblatt, D. and Moss, E.A., "Rapid temporal acceleration of a turbulent pipe flow," *Journal of Fluid Mechanics*, Vol 514, 2004, pp. 65-75. https://doi.org/10.1017/S0022112004000114.
13. He, S., Ariyaratne, C. and Vardy, A.E., "Wall shear stress in accelerating turbulent pipe flow," *Journal of Fluid Mechanics*, Vol. 685, pp. 440-460. https://doi.org/10.1017/jfm.2011.328.
14. Jung, S.Y. and Chung, Y.M., "Large-eddy simulation of accelerated turbulent flow in a circular pipe," *International Journal of Heat and Fluid Flow*, Vol. 33, No. 1, 2012, pp. 1-8. https://doi.org/10.1016/j.ijheatfluidflow.2011.11.005.
15. Talha, T. and Chung, Y.M., "Large-eddy simulations of temporally accelerating turbulent channel flow," *Journal of Turbulence*, Vol. 16, No. 11, 2015, pp. 1091-1113. https://doi.org/10.1080/14685248.2015.1052464.
16. Mathur, A., Gorji, S., He, S., Seddighi, M., Vardy, A.E., O'Donoghue, T. and Pokrajac, D., "Temporal acceleration of a turbulent channel flow," *Journal of Fluid Mechanics*, Vol. 835, 2018, pp. 471-490. https://doi.org/10.1017/jfm.2017.753.
17. Guerrero, B., Lambert, M.F. and Chin, R.C., "Transient dynamics of accelerating turbulent pipe flow," *Journal of Fluid Mechanics*, Vol. 917, 2021, pp. A43-1-27. https://doi.org/10.1017/jfm.2021.303.
18. Narasimha, R. and Sreenivasan, K.R., "Relaminarization in highly accelerated turbulent boundary layers," *Journal of Fluid Mechanics*, Vol. 61, No. 3, 1973, pp. 417-447. https://doi.org/10.1017/S0022112073000790.
19. C. Ariyaratne, S. He, and A. E. Vardy, "Wall friction and turbulence dynamics in decelerating pipe flows," *Journal of Hydraulic Research*, Vol. 48, 2010, pp. 810-821. https://doi.org/10.1080/00221686.2010.525372.
20. M. Seddighi, S. He, P. Orlandi, and A. E. Vardy, "A comparative study of turbulence in ramp-up and ramp-down unsteady flows," *Flow, Turbulence and Combustion*, Vol. 86, 2011, pp. 439-454. https://doi.org/10.1007/s10494-011-9341-4.
21. Mathur, A., "Study of accelerating and decelerating turbulent flows in a channel," Doctoral Dissertation, University of Sheffield, 2016. https://etheses.whiterose.ac.uk/12350/.
22. Guerrero, B., Lambert, M.F. and Chin, R.C., "Transient behaviour of decelerating turbulent pipe flows," *Journal of Fluid Mechanics*, Vol. 962, 2023, pp. A44-1-32. https://doi.org/10.1017/jfm.2023.294.
23. Greenblatt, D., "Unsteady low-speed wind tunnels," *AIAA Journal*, Vol. 54, No. 6, 2016, pp. 1817-1830. https://doi.org/10.2514/1.J054590.

24. Schlichting, H., "Boundary Layer Theory," McGraw-Hill, New York, 1979, pp. 637-644.
25. Lefebvre, P.J. and White, F.M., "Experiments on transition to turbulence in a constant-acceleration pipe flow," *Journal of Fluids Engineering*, Vol. 111, No. 4, 1989, pp. 428-432. https://doi.org/10.1115/1.3243663.
26. Jentzsch, M., Schmidt, H.J., Woszidlo, R., Nayeri, C.N. and Paschereit, C.O., "Challenges and procedures for experiments with steady and unsteady model velocities in a water towing tank," *Experiments in Fluids*, Vol. 62, 2021, pp. 1-20. https://doi.org/10.1007/s00348-021-03151-5.
27. Greenblatt, D. and Moss, E.A., "Rapid transition to turbulence in pipe flows accelerated from rest," *Journal of Fluids Engineering*, Vol. 125, No. 6, 2003, pp.1072-1075. https://doi.org/10.1115/1.1624423.